

# Ion Temperature Gradient Modes in Helical Systems

KURODA Tohru, SUGAMA Hideo<sup>1</sup>, KANNO Ryutaro<sup>1</sup> and OKAMOTO Masao<sup>1</sup>

*Graduate University for Advanced Studies, Toki 509-5292, Japan*

<sup>1</sup>*National Institute for Fusion Science, Toki 509-5292, Japan*

(Received: 18 December 1998 / Accepted: 19 February 1999)

## Abstract

Ion temperature gradient (ITG) modes in helical systems are studied. The gyrokinetic equation for ions, the adiabatic assumption for electrons, and the charge neutrality condition are used with the ballooning representation to derive a kinetic integral equation, which is solved numerically to obtain the linear growth rate, the real frequency, and the eigenfunction of the ITG modes. Using a simple helical field model, cases with  $L = 2$  and  $2 \leq M \leq 10$  are investigated where  $L$  and  $M$  are the poloidal and toroidal polarity numbers characterizing the helical field ripple, respectively. The effects of the toroidal polarity number  $M$  on the dispersion relation and the mode structure of the ITG modes are clarified.

## Keywords:

ITG modes, helical systems, ballooning representation

## 1. Introduction

The ion temperature gradient (ITG) modes are electrostatic drift waves and have been studied as a candidate to explain anomalous heat transport in high temperature plasmas [1]. For toroidal systems such as tokamaks and stellarators, the properties of the ITG modes are significantly affected by the magnetic field geometry through the  $\nabla B$  and curvature drift motion of particles.

For tokamaks, the magnetic field strength is given by the large-aspect-ratio approximation as  $B/B_0 = 1 - \varepsilon_t \cos \theta$  where  $\theta$  is the poloidal angle and  $\varepsilon_t = r/R$  is the inverse aspect ratio representing the toroidal ripple where  $r$  and  $R$  denote the minor and major radii, respectively. Many studies have been done on the ITG modes in tokamaks [2,3,4]. In this case, the ITG modes are confined mostly in the outside of the torus,  $-\pi/2 < \theta < \pi/2$ , which corresponds to the bad curvature region.

For helical systems, the magnetic field strength is approximately given by

$$B/B_0 = 1 - \varepsilon_t \cos \theta - \varepsilon_h \cos(L\theta - M\zeta), \quad (1)$$

where  $\zeta$  is the toroidal angle and the term with  $\varepsilon_h$  in the

right-hand side represents the helical ripple with the poloidal and toroidal polarity numbers denoted by  $L$  and  $M$ , respectively. For example, we have  $L = 2$  and  $M = 10$  for LHD and  $L = 2$  and  $M = 8$  for CHS. Since the helical magnetic ripple affects the particles' drift motion, the properties of the ITG modes stability in helical systems can be different from those in tokamaks [5].

In the present work, we investigate the properties of the ITG modes for the helical systems with  $L = 2$  and  $2 \leq M \leq 10$  which are compared to the tokamak case. Especially, the effects of the toroidal polarity number  $M$  on the dispersion relation and the mode structure of the ITG modes are studied.

## 2. Kinetic ITG Mode Equation for Helical Systems

Here we consider a high-temperature collisionless plasma and assume that, in the presence of the electrostatic perturbation  $\phi$ , the perturbed electron

density is described by the adiabatic (or Boltzmann) response  $\delta n_e = (e\phi/T_e)n_0$ . The perturbed ion distribution function is written as  $\delta f_i = -(e\phi/T_e)n_0 F_M + h \exp(-i \mathbf{k}_\perp \cdot \boldsymbol{\rho})$  where  $F_M \equiv \pi^{-3/2} v_{Ti}^{-3} \exp(-v^2/v_{Ti}^2)$  is the Maxwellian distribution function,  $v_{Ti} \equiv (2T_i/m_i)^{1/2}$  is the thermal velocity for the ions with the mass  $m_i$  and the temperature  $T_i$ ,  $\boldsymbol{\rho} \equiv \mathbf{b} \times \mathbf{v}/\Omega_i$  ( $\mathbf{b} = \mathbf{B}/B$ ) is the ion gyroradius vector, and  $\Omega_i \equiv eB/(m_i c)$  is the ion gyrofrequency. The non-adiabatic part of the distribution function  $h$  is determined by the linear gyrokinetic equation

$$\begin{aligned} & (\omega - \omega_D + i\nu_{\parallel} \mathbf{b} \cdot \nabla) h \\ & = (\omega - \omega_{*T}) \frac{e\phi}{T_i} J_0(k_{\perp} \rho) n_0 F_M. \end{aligned} \quad (2)$$

Here  $\omega$  is the frequency of the perturbation,  $\omega_D = \mathbf{k}_\perp \cdot \mathbf{v}_D$  is the ion  $\nabla B$ -curvature drift frequency,  $J_0$  is the Bessel function of order zero, and  $\omega_{*T} = \omega_{*i} [1 + \eta_i \{(v/v_{Ti})^2 - 3/2\}]$  where  $\eta_i \equiv d \ln T_i / d \ln n_0$  is the ratio of the ion temperature gradient to the density gradient,  $\omega_{*i} \equiv -\tau_e^{-1} \omega_{*e}$  is the ion diamagnetic drift frequency,  $\tau_e \equiv T_e/T_i$  is the ratio between the electron and ion temperatures,  $\omega_{*e} \equiv ck_{\theta} T_e / (eBL_n)$  is the electron diamagnetic drift frequency,  $L_n = -(d \ln n_0 / dr)^{-1}$  is the density gradient scale length, and  $k_{\theta}$  is the poloidal wavenumber.

We use the ballooning representation and write the perpendicular wavenumber vector as  $\mathbf{k}_\perp = k_{\alpha} (\nabla \alpha + \theta_k \nabla q)$  where  $q$  is the safety factor,  $\alpha = \zeta - q\theta$  is the label for magnetic field line, and  $k_{\alpha} = -n$  represents the toroidal mode number, which is related to the poloidal wavenumber as  $k_{\theta} = nq/r$ . In the present work, we assume that  $\theta_k = 0$ . We consider a large aspect-ratio and low  $\beta$  toroidal system and use Eq. (1) to give the ion  $\nabla B$ -curvature drift frequency as

$$\begin{aligned} \omega_D = & 2(L_n/r) \omega_{*i} (v_{\parallel}^2 + v_{\perp}^2/2) v_{Ti}^2 \\ & [\varepsilon_i \{\cos \theta + \hat{s} \theta \sin \theta\} + L\varepsilon_h \{\cos(L\theta - M\zeta) \\ & + \hat{s} \theta \sin \theta (L\theta - M\zeta)\}], \end{aligned} \quad (3)$$

where  $\hat{s} = (r/q) dq/dr$  is the shear parameter.

Neglecting the trapped ions, integrating the gyrokinetic equation (2) along the field line with the boundary conditions  $h(\theta \rightarrow \pm\infty) = 0$ , and substituting it into the charge neutrality condition  $e\phi/T_e = \delta n_e/n_0 = \delta n_i/n_0 = -e\phi/T_i + \int d^3v J_0(k_{\perp} \rho) h$ , we obtain the integral equation which is written as

$$\left(1 + \frac{T_e}{T_i}\right) \phi(k) = \int_{-\infty}^{+\infty} \frac{dk'}{\sqrt{2\pi}} K(k, k') \phi(k'), \quad (4)$$

with

$$\begin{aligned} K(k, k') = & -i \int_{-\infty}^0 \omega_{*e} d\tau \frac{\sqrt{2} e^{-i\omega\tau}}{\sqrt{a}(1+a)\sqrt{\lambda}} e^{-(k-k')^2/4\lambda} \\ & \times \left[ \frac{\omega}{\omega_{*e}} \tau_e + 1 - \frac{3}{2} \eta_i + \frac{\eta_i (k-k')^2}{4a\lambda} \right. \\ & + \frac{2\eta_i}{(1+a)} \left( 1 - \frac{k_{\perp}^2 + k_{\perp}'^2}{2(1+a)\tau_e} \right. \\ & \left. \left. + \frac{k_{\perp} k_{\perp}'}{(1+a)\tau_e} \frac{I_1}{I_0} \right) \right] \Gamma_0(k_{\perp}, k_{\perp}'), \end{aligned} \quad (5)$$

where  $\lambda = (\omega_{*e} \tau)^2 (\hat{s} \varepsilon_n / q)^2 / \tau_e a$ ,  $\theta = k/\hat{s} k_{\theta}$ ,  $\theta' = k'/\hat{s} k_{\theta}$ ,  $\Gamma_0 = I_0(k_{\perp} k_{\perp}' / [(1+a)\tau_e]) \exp[-(k_{\perp}^2 + k_{\perp}'^2)/2I_e(1+a)]$ ,  $k_{\perp}^2 = k_{\theta}^2 + k^2$ ,  $k_{\perp}'^2 = k_{\theta}^2 + k'^2$ , and

$$\begin{aligned} a = & 1 + i2(L_n/r) \tau_e^{-1} \omega_{*e} \tau / (\theta - \theta') \\ & \times (\varepsilon_i [(\hat{s} + 1) (\sin \theta - \sin \theta') \\ & - \hat{s} (\theta \cos \theta - \theta' \cos \theta') \\ & + (L\varepsilon_h / (L - Mq)) \{ \hat{s} / (L - Mq) + 1 \} \\ & \times \{ \sin((L - Mq)\theta - M\alpha) \\ & - \sin((L - Mq)\theta' - M\alpha) \} \\ & - \hat{s} \{ \theta \cos((L - Mq)\theta - M\alpha) \\ & - \theta' \cos((L - Mq)\theta' - M\alpha) \}]). \end{aligned} \quad (6)$$

Here the wavenumber variables  $k_{\theta}$ ,  $k$ , and  $k'$  are normalized by  $\rho_s^{-1}$  ( $\rho_s = \sqrt{2T_e/m_i}/\Omega_i$ ) and  $\varepsilon_h \propto r^L$  is used. The integral equation (4) with the boundary conditions  $\phi(\theta \rightarrow \pm\infty) = 0$  determines the complex-valued eigenfrequency and eigenfunction of the ITG mode for the helical system. If we put  $\varepsilon_h = 0$ , the integral ITG mode equation (4) with Eqs. (5) and (6) reduces to the one given by Dong, *et al.* for the tokamak case [3].

### 3. Numerical Results

Here we numerically solve the integral equation (4) with the boundary conditions  $\phi(\theta \rightarrow \pm\infty) = 0$  to obtain the growth rate, the real frequency, and the eigenfunction of the ITG mode for the  $L = 2$  helical systems with various  $M$  numbers. Since we are concerned with the effects of the helical ripple, we neglect the toroidal ripple by putting  $\varepsilon_i = 0$  (straight helical system) for simplicity. Typical parameters used here are  $q = 2$ ,  $k_{\theta} \rho_{Ti} = 0.75$ ,  $T_i/T_e = 1$ ,  $L_n/R_0 = 0.2$ ,  $L_n \varepsilon_h/r = 0.2$ , and  $\hat{s} = -1$  (negative shear). We also treat a single field line labelled by  $\alpha = 0$ .

Figure 1 shows the normalized real frequency  $\omega_r/\omega_{e*}$  and growth rate  $\omega_i/\omega_{e*}$  of the ITG mode as a function of  $M$  for  $\eta_i = 3, 4, 6, 8$ . Other parameters used here are the same as mentioned above. The real frequencies obtained here are all negative, which corresponds to the ion diamagnetic rotation. The growth rate decreases with increasing  $M$ .

Corresponding to the cases for  $M = 2, 3, 4, 5, 8, 10$  in Fig. 1, the profiles of the eigenfunction and the helical drift frequency  $\propto \cos[(L - Mq)\theta] + \hat{s} \sin[(L - Mq)\theta]$  in the covering space ( $\theta$ -space) are plotted in Fig. 2. The regions where the helical drift frequency is positive (negative) corresponds to bad (good) curvature. As  $M$  increases, the eigenfunction  $\phi$  becomes more rippled in the covering space and has a larger amplitude in the good curvature region, which is related to the reduction of the growth rate for larger  $M$ .

In the cases with large  $M$  like  $M = 8$  (CHS) and  $M = 10$  (LHD), a positive growth rate for the ITG mode cannot be found for  $\eta_i < 4$ , with the other parameters as given above. Unstable ITG modes are found for  $M = 8$  and 10 with the very large temperature gradient (or very small density gradient)  $\eta_i = 6, 8$  and they have more negative frequencies and more rippled eigenfunctions as shown in Figs. 1 and 2.

#### 4. Conclusions

In the present paper, we have derived a kinetic integral equation for the ITG modes in helical systems. The ITG mode equation was numerically solved for a straight helical system with the poloidal polarity number  $L = 2$ , and the effects of the toroidal polarity number  $M$  on the dispersion relation and the mode structure of the ITG mode were studied. Field ripple with larger  $M$  reduces the growth rate of the ITG mode. This stabilizing effect is understood based on the structure of the eigenfunction along the field line as follows. As  $M$  increases, the connection length between the good and bad curvature regions becomes shorter and the eigenfunction invades the good curvature region, which leads to the stabilization.

In this work, the toroidal ripple in the magnetic field strength, the nonadiabatic electrons, and the trapped ions are not considered. These effects on the properties of the ITG modes are studied as a future task.

#### Acknowledgments

The authors thank Dr. Rewoldt for his careful reading of the manuscript and useful comments. This work is supported in part by a Grant-in-Aid from the

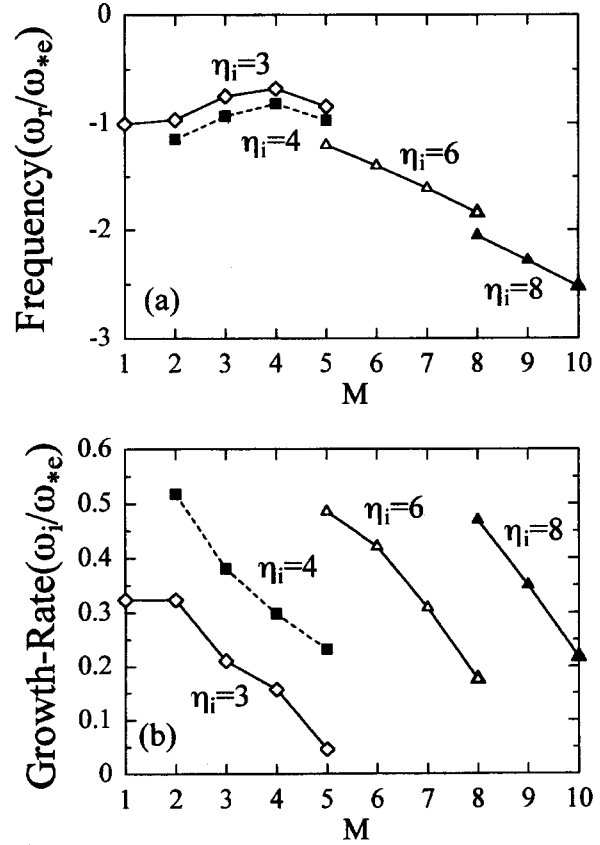


Fig. 1 The normalized (a) real frequency  $\omega_r/\omega_{e*}$  and (b) growth rate  $\omega_i/\omega_{e*}$  of the ITG mode as a function of  $M$  for various  $\eta_i$ 's. Here  $q = 2$ ,  $k_0 \rho_{Ti} = 0.75$ ,  $T_i/T_e = 1$ ,  $L_n/R_0 = 0.2$ ,  $L_n \varepsilon_h/r = 0.2$ ,  $\varepsilon_i = 0$ , and  $\hat{s} = -1$ .

Japanese Ministry of Education, Science and Culture.

#### References

- [1] W. Horton, M. Wakatani, and J.A. Wooton, *AIP Conf. Proc. 284, U.S.-Japan Workshop on Ion Temperature Gradient-Driven Turbulent Transport*, New York: AIP, 1994, ch. 1, p. 3.
- [2] F. Romanelli, *Phys. Fluids B* **1**, 1018 (1989).
- [3] J.Q. Dong, W. Horton, and J.Y. Kim, *Phys. Fluids B* **4**, 1867 (1992).
- [4] J.Q. Dong and W. Horton, *Phys. Fluids B* **5**, 1581 (1993).
- [5] J.L.V. Lewandowski, *Plasma Phys. Control. Fusion* **40**, 283, (1998).

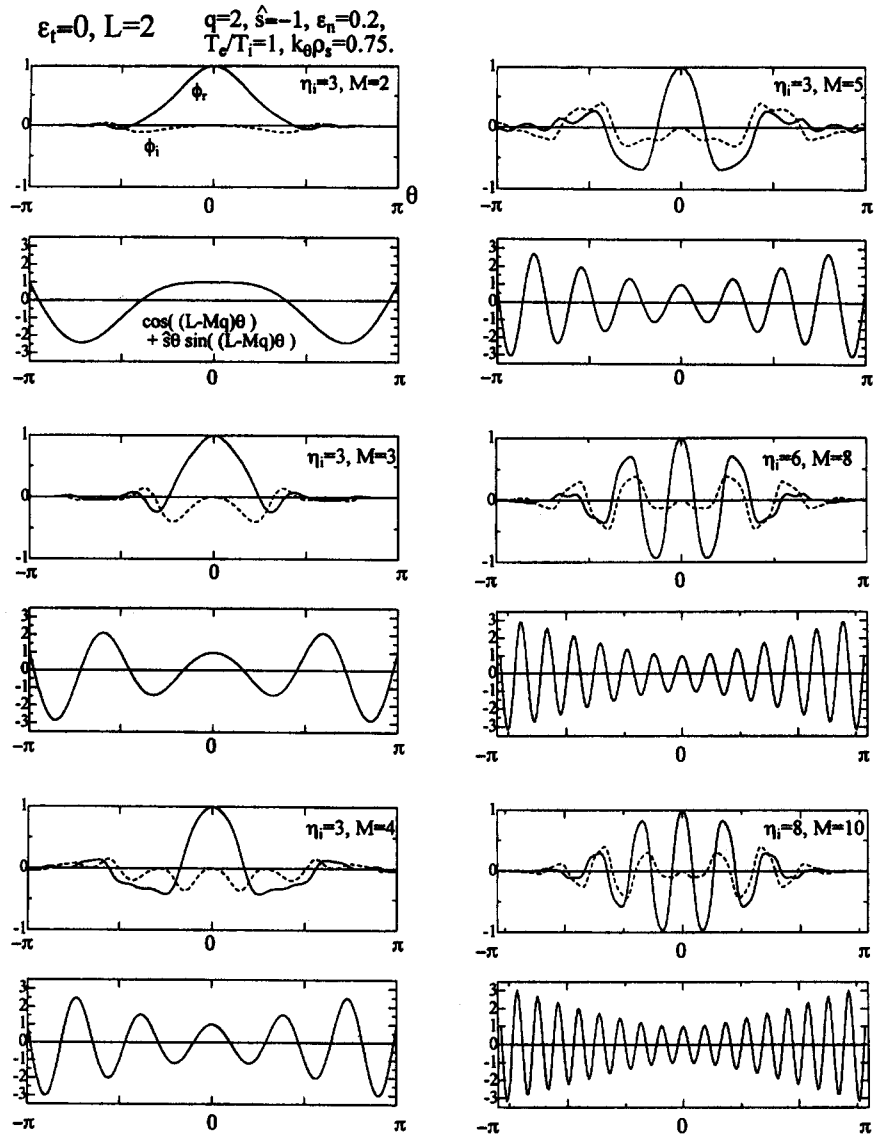


Fig. 2 The profiles of the eigenfunction  $\phi$  and the helical drift frequency  $\propto \cos[(L - Mq)\theta] + \hat{s}\theta \sin[(L - Mq)\theta]$  in the covering space ( $\theta$ -space) for  $M = 2, 3, 4, 5, 8, 10$ . Other parameters are the same as in Fig. 1.